GALAXY FEEDBACK

Fast molecular outflow from a dusty star-forming galaxy in the early Universe

J. S. Spilker[1,2]*, M. Aravena[3], M. Béthermin[4], S. C. Chapman[5], C.-C. Chen[6], D. J. M. Cunningham[5,7], C. De Breuck[6], C. Dong[8], A. H. Gonzalez[8], C. C. Hayward[9,10], Y. D. Hezaveh[11], K. C. Litke[2], J. Ma[12], M. Malkan[13], D. P. Marrone[2], T. B. Miller[5,14], W. R. Morningstar[11], D. Narayanan[8], K. A. Phadke[15], J. Sreevani[15], A. A. Stark[10], J. D. Vieira[15], A. Weiß[16]

Galaxies grow inefficiently, with only a small percentage of the available gas converted into stars each free-fall time. Feedback processes, such as outflowing winds driven by radiation pressure, supernovae, or supermassive black hole accretion, can act to halt star formation if they heat or expel the gas supply. We report a molecular outflow launched from a dust-rich star-forming galaxy at redshift 5.3, 1 billion years after the Big Bang. The outflow reaches velocities up to 800 kilometers per second relative to the galaxy, is resolved into multiple clumps, and carries mass at a rate within a factor of 2 of the star formation rate. Our results show that molecular outflows can remove a large fraction of the gas available for star formation from galaxies at high redshift.

The formation of realistic populations of galaxies requires one or more forms of self-regulating feedback to suppress the conversion of gas into stars. Cosmological simulations invoke various mechanisms to regulate star formation, in the form of energy deposition and wind launching linked to supermassive black hole activity, supernovae, and/or radiation pressure from massive stars. The strength and scalings of these processes play critical roles in the evolution of galaxies by regulating the growth of stellar mass relative to the dark-matter halo, connecting the properties of central black holes to their host galaxies, and enriching the circumgalactic medium with heavy elements (*1*–*4*).

Outflowing winds of gas are ubiquitous in nearby galaxies. The gas in outflows spans many orders of magnitude in temperature and density (*5*–*7*), and different components of the winds are observable from x-ray to radio wavelengths. Observing winds in the distant Universe is difficult: Not only are the spectral features faint, but outflow tracers observed in emission may be less reliable because of the ongoing processes of galaxy assembly (*8*). The constrained geometry of absorption lines provides signatures of inflowing and outflowing material, but these lines have thus far eluded detection.

Passive galaxies with stellar masses of ~10^{11} $M_\odot$ (where $M_\odot$ is the solar mass), low star formation rates (SFRs) ($\lesssim 10 M_\odot$ yr^{-1}), and stellar ages of ~0.8 billion years were already in place when the Universe was 2 billion years old, implying that these galaxies formed stars at rates of hundreds of $M_\odot$ per year before $z = 5$ (where z is the redshift) (*9*). Galaxies with such high SFRs are extremely rare in rest-ultraviolet surveys, implying that such galaxies are incapable of becoming sufficiently massive by $z \sim 4$ to reproduce the observed passive population. This suggests a connection between early passive galaxies and high-redshift dusty star-forming galaxies (DSFGs) observed at far-infrared wavelengths (*10*–*12*). With a redshift distribution that includes a substantial number of objects at $z > 4$ (*13*, *14*), DSFGs represent a plausible progenitor population of the earliest passive galaxies. If this evolutionary connection is correct, many DSFGs should show signs of the feedback process(es) acting to suppress their rapid star formation.

We present observational evidence of a massive molecular wind being launched from SPT–S J231921–5557.9 (hereinafter referred to as SPT2319–55), a DSFG observed when the Universe was only 1 billion years old. SPT2319–55 was discovered in the 2500-square-degree South Pole Telescope survey (*15*) on the basis of its thermal dust emission. Earlier observations of this source from the Atacama Large Millimeter/submillimeter Array (ALMA) determined its redshift to be $z_{\rm source} = 5.293$ (*14*) and showed that it is gravitationally lensed by an intervening foreground galaxy (*16*). As is typical for these objects, SPT2319–55 is gas rich, containing ~1.2×10^{10} $M_\odot$ of molecular gas and ~1.2×10^{8} $M_\odot$ of dust, and is forming stars very rapidly, with an SFR of ~790 $M_\odot$ yr^{-1} (*17*) (these values account for the lensing magnification).

We used ALMA to observe the rest-frame 119-μm ground-state doublet transition of the hydroxyl molecule, OH, and the thermal dust emission at this wavelength (*17*). This transition is a good tracer of gas flows in nearby galaxies (*18*, *19*). The ALMA observations reach a spatial resolution of 0.25 by 0.4 arc sec and resolve the lensed images of SPT2319–55 (Fig. 1). We detected a molecular outflow from SPT2319–55, seen in blueshifted absorption against the bright dust continuum emission, a signature of outflowing molecular material (Fig. 1).

We fit the spectrum in Fig. 1 with the sum of two velocity components, each consisting of two equal-amplitude Gaussian profiles separated by 520 km s^{-1}, the separation of the two components of the OH doublet (*17*). As is common practice for low-redshift observations of OH, we assigned the higher-frequency component of the doublet to the systemic velocity of the galaxy. Because the redshift of this source is known to better than 50 km s^{-1} from other observations (*14*), we fixed the velocity offset of one pair of Gaussian profiles to the systemic velocity. This component represents absorption due to gas from within the galaxy, with a fitted full-width-at-half-maximum (FWHM) linewidth of 330 ± 80 km s^{-1}. We allowed a velocity offset for the second pair of Gaussian profiles; this component represents the blueshifted molecular outflow. We found that this second component is blueshifted relative to the galaxy by 440 ± 50 km s^{-1} and derived a maximum velocity of ~800 km s^{-1} (*17*).

The ALMA observations spatially resolve and clearly detect the dust continuum even in relatively narrow velocity channels. Because SPT2319–55 is gravitationally lensed by a foreground galaxy, we determine its intrinsic structure by using a lens modeling technique that represents the galaxy as an array of pixels (*17*, *20*). In addition to the line-free continuum emission, we also reconstructed the OH absorption components by using velocity ranges relative to the higher-frequency OH transition of −700 to −200 km s^{-1} for the wind component and +300 to +700 km s^{-1} for the internal component; the latter velocity range corresponds to velocities of −220 to +180 km s^{-1} relative to the lower-frequency transition and traces gas within SPT2319–55. These

[1]Department of Astronomy, University of Texas at Austin, 2515 Speedway Stop C1400, Austin, TX 78712, USA. [2]Steward Observatory, University of Arizona, 933 North Cherry Avenue Tucson, AZ 85721, USA. [3]Núcleo de Astronomía, Facultad de Ingeniería, Universidad Diego Portales, Av. Ejército 441, Santiago, Chile. [4]Aix Marseille Univ., Centre National de la Recherche Scientifique, Laboratoire d'Astrophysique de Marseille, Marseille, France. [5]Department of Physics and Atmospheric Science, Dalhousie University, Halifax, Nova Scotia, Canada. [6]European Southern Observatory, Karl Schwarzschild Straße 2, 85748 Garching, Germany. [7]Department of Astronomy and Physics, Saint Mary's University, Halifax, Nova Scotia, Canada. [8]Department of Astronomy, University of Florida, Bryant Space Sciences Center, Gainesville, FL 32611, USA. [9]Center for Computational Astrophysics, Flatiron Institute, 162 Fifth Avenue New York, NY 10010, USA. [10]Harvard-Smithsonian Center for Astrophysics, 60 Garden St., Cambridge, MA 02138, USA. [11]Kavli Institute for Particle Astrophysics and Cosmology, Stanford University, Stanford, CA 94305, USA. [12]Department of Physics and Astronomy, University of California, Irvine, CA 92697, USA. [13]Department of Physics and Astronomy, University of California, Los Angeles, CA 90095, USA. [14]Department of Astronomy, Yale University, 52 Hillhouse Avenue New Haven, CT 06511, USA. [15]Department of Astronomy, University of Illinois, 1002 West Green Street Urbana, IL 61801, USA. [16]Max-Planck-Institut für Radioastronomie, Auf dem Hügel 69, D-53121 Bonn, Germany.
*Corresponding author. Email: spilkerj@gmail.com

velocity ranges fairly cleanly separate the wind and internal absorption (*17*).

The doubly-imaged continuum emission in Fig. 1 is consistent with the lensing of a single background galaxy, with a well-determined extent, by a single foreground lens. The reconstructions of the dust continuum and each absorption component are shown in Fig. 2. The continuum is dominated by a single bright region ~1.2 kpc in diameter (*17*), with flux density $S_{400\mathrm{GHz}}$ = 9.0 mJy (1 Jy = 10^{-26} W m^{-2} Hz^{-1}) magnified by a factor μ = 5.8. The internal absorption, arising from gas within the galaxy, is concentrated toward the center of the object. This is to be expected, as the continuum is brightest and gas column densities are highest toward the nuclear region, making the detection of absorption easier.

The geometry of the molecular outflow is more complex and is not confined to the center of the galaxy. Instead, it is clustered into multiple clumps, separated from each other by a few hundred parsecs, corresponding to ≈2.5 FWHM resolution elements (*17*). Because absorption is easier to detect against a strong continuum, we would expect a geometry similar to that of the internal absorption if the continuum were the limiting factor in the reconstruction. Tests using mock data also show that absorbing components weaker than the outflow are well recovered by our reconstructions (*17*).

The overall covering fraction of the wind is high—80% of pixels with a continuum signal-to-noise ratio of >8 have significant wind absorption (although these pixels are not all independent) (*17*). If the covering fraction along the line of sight we observe is the same as that for the rest of the source, this implies a total wind opening angle of ~$0.8 \times 4\pi$ sr. On the other hand, we can set a rough lower limit on the opening angle if we assume that we have observed the entirety of the outflow and that the molecular material is destroyed by the time it reaches a few galaxy radii away, as in local starburst galaxies (*6*). If the maximum radius of the outflowing material is 2 galaxy radii, for example, then the solid angle of a sphere of this radius subtended by the source is $(\pi r_{\mathrm{eff}}^2)/\left(4\pi(2r_{\mathrm{eff}})^2\right) \times 4\pi$ sr, with r_{eff} representing the radius of the galaxy. With an 80% covering fraction of the source along the line of sight, this implies a minimum opening angle of 0.2π sr.

In low-redshift galaxies, the 119-μm OH transitions are very optically thick (*21*), and the absorption depth thus directly corresponds to the covering fraction of the continuum. The difference between the 80% covering fraction from our lens modeling and the peak wind depth (~15%) mirrors the discrepancy between the typical absorption depths and the high detection rate of

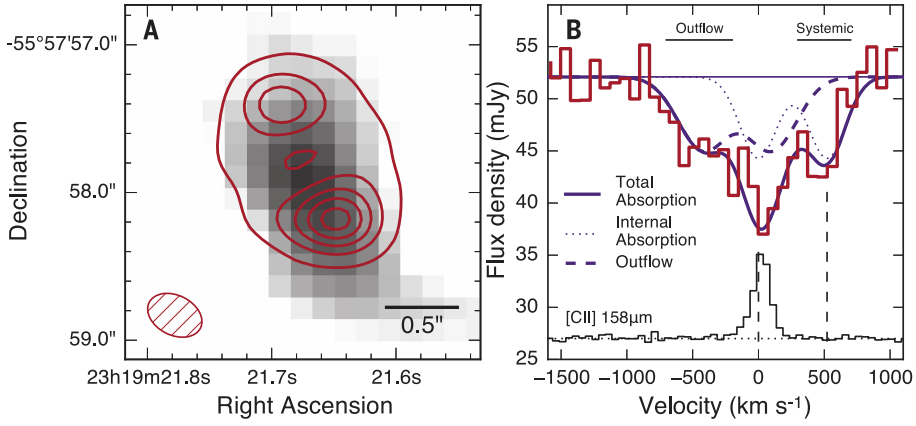

Fig. 1. ALMA 400-GHz continuum image and OH spectrum of SPT2319−55. (**A**). The ALMA continuum data (red contours) overlaid on a 2.2-μm image of the foreground lens galaxy. Contours are drawn at 10, 30, 50, 70, and 90% of the peak value; the data reach a peak signal-to-noise ratio of ~140. The synthesized beam is shown by a striped ellipse at the lower left. (**B**) The integrated apparent (not corrected for lensing magnification) OH 119-μm spectrum of SPT2319−55, with the velocity scale relative to the higher-frequency component of the OH doublet. The rest velocities of the two doublet components are shown with vertical dashed lines, and we show an ALMA [CII] spectrum of this source (*17*) as an indication of the linewidth of this galaxy due to internal gas motions (with arbitrary vertical normalization). We fit the OH 119-μm spectrum as described in the text; the navy dotted line shows the component due to gas within the galaxy, the navy dashed line the blueshifted outflow component, and the navy solid line the total absorption profile. We mark the velocity ranges for which we created lens models with horizontal bars above the continuum.

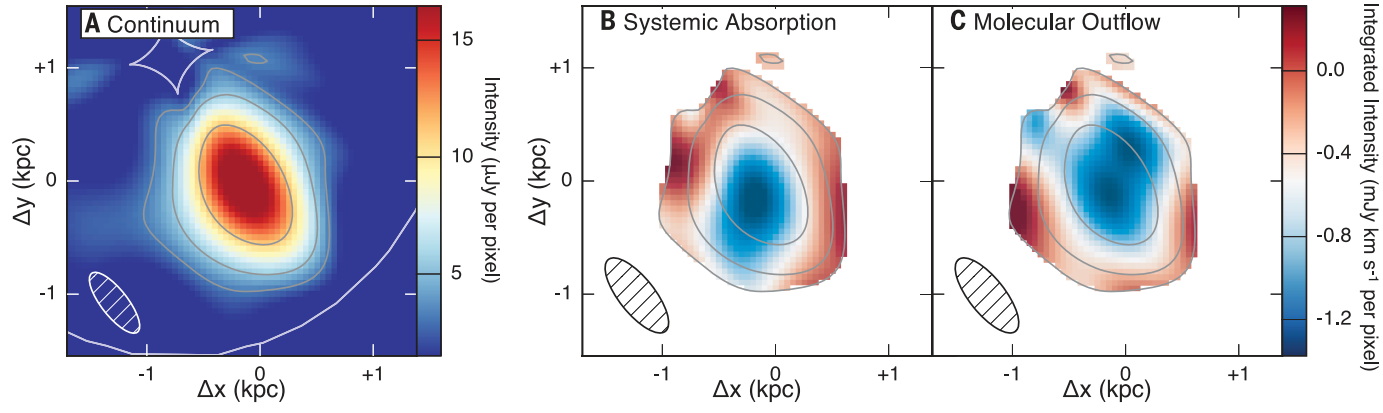

Fig. 2. Lensing reconstruction of the continuum and OH absorption in SPT2319−55. (**A**) Source-plane structure of the rest-frame 119-μm continuum emission after modeling of the effects of gravitational lensing. Contours are shown at signal-to-noise ratios of 8, 16, and 32; these contours are repeated in subsequent panels. The ellipse at the lower left shows the effective resolution of the reconstruction (*17*). The lensing caustics (lines of theoretically infinite magnification) are also shown. Coordinates are offset relative to the ALMA phase center. (**B**) Reconstruction of the absorption due to gas internal to SPT2319−55. (**C**) Reconstruction of the molecular outflow. Because the reconstruction of the absorption requires the presence of continuum emission, in panels (B) and (C) we mask pixels with a continuum signal-to-noise ratio of <8. We separate the internal and outflow absorption by using the velocity ranges labeled in Fig. 1. Ellipses at the lower left indicate the effective spatial resolution of the absorption reconstructions (*17*).

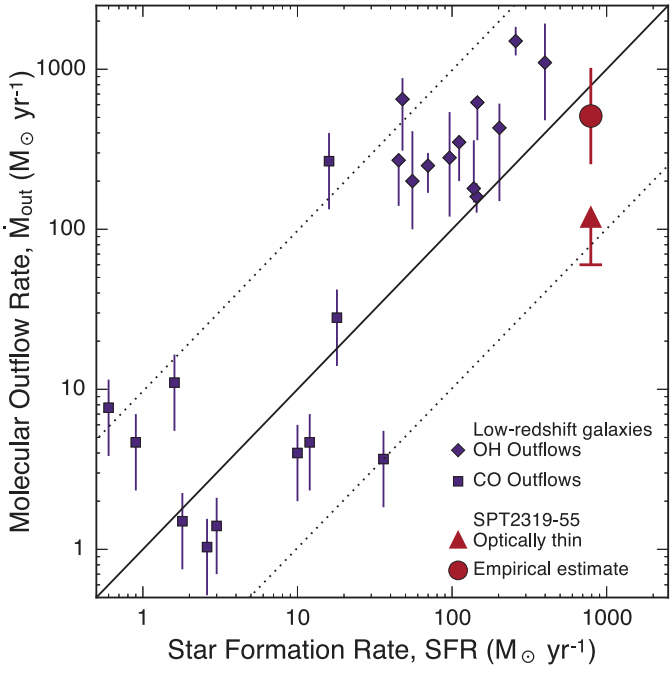

Fig. 3. Molecular outflow rates as a function of the star formation rate. Outflow rates are from both OH and CO (*21*, *23*). The solid line shows the one-to-one relation, with dotted lines representing a factor of 10 above and below. The low-redshift samples include both sources dominated by star formation and sources with active galactic nuclei. Error bars show estimated standard uncertainties on the measurements.

winds in low-redshift objects studied in OH (*19*, *22*). If the OH absorption in SPT2319–55 is also optically thick, we expect that the wind contains substantial substructure on scales below our effective resolution limit, with most of the absorption arising from small, highly optically thick clumps. Alternatively, because the outflow reconstruction spans a wide range of velocities, it is possible that the covering fraction is lower in narrower velocity ranges. In this case, we also expect substantial substructure on smaller scales, as the lower covering fractions in narrow velocity bins must still sum to the high overall covering fraction we have observed. On the other hand, if the OH excitation temperature is high, the OH molecules can substantially fill in the absorption profile with re-emitted 119-μm photons, reducing the absorption strength while maintaining a high covering fraction without small-scale structure in the wind, although this implies high densities in the absorbing gas.

We estimated the mass outflow rate by using a simple model for the outflow geometry (*17*). The primary uncertainties in this estimate are the unknown optical depth of the OH 119-μm doublet and the detailed geometry of the wind. In the limiting case of optically thin absorption, we find a minimum mass outflow rate $\dot{M}_{out} \gtrsim 60\,M_\odot\,yr^{-1}$. A more likely outflow rate, on the basis of the empirical correlation between the OH equivalent width and $\dot{M}_{out}$ in low-redshift dusty galaxies (*17*), is $\dot{M}_{out} \sim 510\,M_\odot yr^{-1}$. Though highly uncertain (*17*), this value is within a factor of 2 of the SFR of SPT2319–55, indicating that the wind is capable of depleting the molecular gas reservoir on a time scale similar to that of star formation itself. We compare the SFR and molecular outflow rates we derived for SPT2319–55 under both assumptions in Fig. 3, along with molecular outflow rates for low-redshift objects (*21*, *23*).

The mass loading factor of the wind, $\dot{M}_{out}/SFR \sim 0.7$, is high, even accounting for molecular material alone; the inclusion of unobserved wind phases, namely, neutral atomic and ionized gases, would increase this value still further. High mass loading factors are expected from simulations of galaxies (*24*, *25*), which require strong feedback to prevent the overproduction of stars. On the other hand, both the origin of the molecules in the SPT2319–55 wind (whether entrained in hotter material or formed in situ) and the driving source are unclear. Current data place an upper limit of 30% on the contribution of an active galactic nucleus to the total luminosity of SPT2319–55 but cannot rule out nuclear activity at a lower level (*17*).

Despite the high overall outflow rate, it is likely that only a small fraction of the wind mass is sufficiently fast-moving to escape the gravitational potential of the galaxy. Given the molecular gas mass of SPT2319–55, assuming a typical gas fraction for DSFGs at this redshift (*26*) and using the size from the source reconstruction yield an escape velocity from the galaxy of ~650 km s^{-1}. The fraction of the absorption at speeds greater than this value indicates that ~10% of the outflowing material will escape SPT2319–55, under the same assumptions as those for the outflow as a whole. This escape fraction is within the range observed in local galaxies (*27*). The remainder of the material, therefore, will stay within the galaxy's dark-matter halo.

Our results show that self-regulating feedback is acting to disrupt and remove the molecular gas in SPT2319–55 and will likely suppress the rapid star formation in this galaxy in $\lesssim$100 million years. Whether this is sufficient to quench the star formation on a more permanent basis is less clear. A large fraction of the wind material is likely to remain within the galaxy, capable of fueling future star formation at later times. On the other hand, SPT2319–55 likely resides in a dark-matter halo of mass ~$10^{12}\,M_\odot$ (*28*), sufficiently massive to shock infalling gas to high temperatures and prevent its accretion (*29*). Other forms of feedback, such as from an active galactic nucleus, may also act to maintain the low SFR after the initial suppression (*30*). Molecular outflows like the one we have observed are likely an important step in the suppression of star formation and the emergence of early passive galaxies.

REFERENCES AND NOTES

1. N. Murray, E. Quataert, T. A. Thompson, *Astrophys. J.* **618**, 569–585 (2005).
2. P. F. Hopkins, L. Hernquist, T. J. Cox, D. Kereš, *Astrophys. J.* **175** (suppl.), 356–389 (2008).
3. J. Kormendy, L. C. Ho, *Annu. Rev. Astron. Astrophys.* **51**, 511–653 (2013).
4. D. Ceverino *et al.*, *Mon. Not. R. Astron. Soc.* **457**, 2605–2612 (2016).
5. S. Veilleux, G. Cecil, J. Bland-Hawthorn, *Annu. Rev. Astron. Astrophys.* **43**, 769–826 (2005).
6. A. K. Leroy *et al.*, *Astrophys. J.* **814**, 83 (2015).
7. E. E. Schneider, B. E. Robertson, *Astrophys. J.* **834**, 144 (2017).
8. D. Narayanan *et al.*, *Nature* **525**, 496–499 (2015).
9. C. M. S. Straatman *et al.*, *Astrophys. J.* **783**, L14 (2014).
10. A. W. Blain, S. C. Chapman, I. Smail, R. Ivison, *Astrophys. J.* **611**, 725–731 (2004).
11. L. J. Tacconi *et al.*, *Astrophys. J.* **680**, 246–262 (2008).
12. K. Glazebrook *et al.*, *Nature* **544**, 71–74 (2017).
13. J. D. Vieira *et al.*, *Nature* **495**, 344–347 (2013).
14. M. L. Strandet *et al.*, *Astrophys. J.* **822**, 80 (2016).
15. L. M. Mocanu *et al.*, *Astrophys. J.* **779**, 61 (2013).
16. J. S. Spilker *et al.*, *Astrophys. J.* **826**, 112 (2016).
17. See supplementary materials.
18. E. Sturm *et al.*, *Astrophys. J.* **733**, L16 (2011).
19. S. Veilleux *et al.*, *Astrophys. J.* **776**, 27 (2013).
20. Y. D. Hezaveh *et al.*, *Astrophys. J.* **823**, 37 (2016).
21. E. González-Alfonso *et al.*, *Astrophys. J.* **836**, 11 (2017).
22. H. W. W. Spoon *et al.*, *Astrophys. J.* **775**, 127 (2013).
23. C. Cicone *et al.*, *Astron. Astrophys.* **562**, A21 (2014).
24. A. L. Muratov *et al.*, *Mon. Not. R. Astron. Soc.* **454**, 2691–2713 (2015).
25. C. C. Hayward, P. F. Hopkins, *Mon. Not. R. Astron. Soc.* **465**, 1682–1698 (2017).
26. M. Aravena *et al.*, *Mon. Not. R. Astron. Soc.* **457**, 4406–4420 (2016).
27. K. Alatalo, *Astrophys. J.* **801**, L17 (2015).
28. P. S. Behroozi, R. H. Wechsler, C. Conroy, *Astrophys. J.* **770**, 57 (2013).
29. A. Dekel, Y. Birnboim, *Mon. Not. R. Astron. Soc.* **368**, 2–20 (2006).
30. A. C. Fabian, *Annu. Rev. Astron. Astrophys.* **50**, 455–489 (2012).

ACKNOWLEDGMENTS

We gratefully acknowledge the allocation of computer time from UA High Performance Computing at the University of Arizona, and we thank the Texas Advanced Computing Center (TACC) at the University of Texas at Austin for providing high-performance computing resources that have contributed to the results reported here. **Funding:** ALMA is a partnership of ESO (representing its member states), the NSF (USA), and NINS (Japan), together with the NRC (Canada) and NSC and ASIAA (Taiwan), in cooperation with the Republic of Chile. The Joint ALMA Observatory is operated by ESO, AUI/NRAO, and NAOJ. The South Pole Telescope is supported by the NSF through grant PLR-1248097, with partial support through PHY-1125897, the Kavli Foundation, and Gordon and Betty Moore Foundation grant GBMF 947. The Australia Telescope Compact Array is part of the Australia Telescope National Facility, which is funded by the Australian government for operation as a National Facility

managed by CSIRO. J.S.S. thanks the McDonald Observatory at the University of Texas at Austin for support through a Smith fellowship. J.S.S., K.C.L., D.P.M., J.S., and J.D.V. acknowledge support from the NSF under grant AST-1312950; K.C.L. and D.P.M. also acknowledge support under AST-1715213, and J.S. and J.D.V. also acknowledge support under AST-1716127. C.C.H. acknowledges support from the Flatiron Institute, which is supported by the Simons Foundation. Y.D.H. is a Hubble fellow.
Author contributions: J.S.S. proposed the ALMA OH observations, performed the data reduction and lensing analysis, and wrote the manuscript. D.P.M. and K.C.L. led the observations of [CII] shown in Fig. 1. M.A. led the CO observations used to calculate the molecular gas mass. K.A.P. and J.D.V. performed modeling of the source spectral energy distribution. All authors discussed the results and provided comments on the figures and text. Authors are ordered alphabetically after J.S.S. **Competing interests:** The authors declare no competing interests. **Data and materials availability:** This paper makes use of the following ALMA data: ADS/JAO.ALMA#2016.1.00089.S and ADS/JAO.ALMA#2016.1.01499.S, archived at https://almascience.nrao.edu/alma-data/archive. Pixelated reconstructions were performed by using a lens modeling tool developed by a subset of the authors and additional non-authors. Developers of this tool include authors Y.D.H. and W.R.M. and non-authors N. Dalal, G. Holder, and P. Marshall. A binary executable version of the lensing tool is provided at https://github.com/yasharhezaveh/Ripple/releases. Reduced data products, lens tool data files, and lensing reconstructions are provided at https://github.com/jspilker/s18_outflow.

SUPPLEMENTARY MATERIALS

www.sciencemag.org/content/361/6406/1016/suppl/DC1
Materials and Methods
Figs. S1 to S8
Tables S1 and S2
References (*31*–*61*)

3 October 2017; accepted 13 July 2018
10.1126/science.aap8900

Fast molecular outflow from a dusty star-forming galaxy in the early Universe

J. S. Spilker, M. Aravena, M. Béthermin, S. C. Chapman, C.-C. Chen, D. J. M. Cunningham, C. De Breuck, C. Dong, A. H. Gonzalez, C. C. Hayward, Y. D. Hezaveh, K. C. Litke, J. Ma, M. Malkan, D. P. Marrone, T. B. Miller, W. R. Morningstar, D. Narayanan, K. A. Phadke, J. Sreevani, A. A. Stark, J. D. Vieira and A. Weiß

Science **361** (6406), 1016-1019.
DOI: 10.1126/science.aap8900

Molecular gas ejected from a distant galaxy

Galaxies grow by forming stars from cold molecular gas. The rate at which they do so is limited by various feedback processes (such as supernovae or stellar winds) that heat and/or eject gas from the host galaxy. Spilker *et al.* used submillimeter observations to discover an outflow of molecular gas from a galaxy in the early Universe, a period of vigorous star formation. Modeling the outflow revealed that the mass of gas being ejected is similar to that being turned into stars. The results will help determine how quickly galaxies formed after the Big Bang.

Science, this issue p. 1016